Reaction dynamics of the $D^+ + H_2$ system. A comparison of theoretical approaches

P. G. Jambrina,[ab] J. M. Alvariño,[a] F. J. Aoiz,*[b] Víctor J. Herrero[c] and Vicente Sáez-Rábanos[d]

Received 21st April 2010, Accepted 15th June 2010
DOI: 10.1039/c0cp00311e

The dynamics of the deuteron–proton exchange $D^+ + H_2 \rightarrow HD + H^+$ reaction on its ground $1^1A'$ potential energy surface has been the subject of a theoretical study for collision energies below 1.5 eV. The results obtained with three theoretical approaches: quasi-classical trajectory (QCT), statistical quasi-classical trajectory (SQCT), and accurate time-independent quantum mechanical (QM) calculations are compared in the range of collision energies from 5 meV to 0.2 eV. The QM calculations included all total angular momentum quantum numbers, J, up to $J_{max} \approx 40$ and all the Coriolis couplings. For higher collision energies, the comparison was restricted to the QCT and SQCT results given the enormous computational cost implied in the QM calculations. Reaction cross sections as a function of collision energy (excitation functions) for various initial rovibrational states have been determined and compared with the corresponding results for the endothermic $H^+ + D_2 \rightarrow HD + D^+$ isotopic variant. The excitation function for the title reaction decays monotonically with collision energy as expected for an exothermic reaction without a barrier, in contrast to the behaviour observed in the mentioned $H^+ + D_2$ ($v = 0, j \leq 3$). Reaction probabilities as a function of J (opacity functions) at several collision energies calculated with the different approaches were also examined and important differences between them were found. The effect of using the Gaussian binning procedure that preserves, to a large extent, the zero point energy, as compared to the standard histogram binning in the QCT calculations, is also examined. At low collision energy, the best agreement with the accurate QM results is given by the SQCT data, although they tend to overestimate the reactivity. The deviations from the statistical behaviour of the QCT data at higher energies are remarkable. Nevertheless, on the whole, the title reaction can be deemed more statistical than the $H^+ + D_2$ reaction.

I. Introduction

Chemical reactions between molecules and ions, excited atoms or radicals are often barrierless and consequently very fast even at low temperature. They play an important role in plasmas or combustion media and are decisive for the very low temperature gas-phase chemistry of interstellar space. In general, this type of reaction is mediated by long-range attractive interactions and proceeds through the formation of an intermediate, more or less long-lived, complex supported by a potential energy well in the path between reactants and products. These characteristics have allowed the formulation of popular and successful capture models and statistical treatments of the kinetics,[1–5] but have hampered the application of rigorous, 'exact' quantum mechanical methods for dynamical investigations, which are rendered particularly difficult by the profusion of channels associated with bound states in the potential well. The simplest system featuring the just mentioned properties is the $H^+ + H_2$ reaction, with only three nuclei and two electrons. Not surprisingly, this system has been the object of extensive experimental and theoretical investigations over the past decades.[6–43] For collision energies, E_{coll}, lower than $\approx$1.8 eV, proton exchange is the only reactive pathway open and we will restrict our attention to this channel. The reaction takes place through the formation of a H_3^+ complex, sustained on a potential well with an approximate depth of 4.5 eV. The H_3^+ molecule is the major ionic constituent of many cold hydrogen plasmas[44,45] and is paramount for the chemistry of interstellar clouds, where it acts as an initiator of protonation chains leading to a large variety of chemical species.[46,47] Although the $H^+ + H_2$ proton exchange reaction is barrierless and thermoneutral, some of its deuterated variants, such as $H^+ + D_2 \rightarrow D^+ + HD$, are endoergic due to the different zero point energies of reactants and products and have thus an energetic threshold that can be very relevant for the low temperatures of interstellar environments.[48–51]

Early theoretical works on the reaction dynamics of the H_3^+ system, carried out using empirical potential surfaces (PES) and quasiclassical trajectories (QCT), indicated that the

[a] *Grupo de Dinámica Molecular, Departamento de Química Física, Facultad de Ciencias Químicas, Universidad de Salamanca, 37008 Salamanca*
[b] *Departamento de Química Física, Facultad de Química, Universidad Complutense, 28040 Madrid, Spain. E-mail: aoiz@quim.ucm.es*
[c] *Instituto de Estructura de la Materia (CSIC), Serrano 123, 28006 Madrid, Spain*
[d] *Departamento de Química y Bioquímica, ETS Ingenieros de Montes, Universidad Politécnica, 28040 Madrid, Spain*

reactivity cannot be fully explained with purely statistical arguments. Direct type short-lived collisions were also found to contribute to the reactivity with an increasing relative weight for growing translational energy.[7–11,13,17–19] These results showed that the formation of a long-lived complex required not only the overcoming of the centrifugal barrier, and therefore experiencing a negative potential, but also an effective momentum transfer of the ionic projectile in its initial encounter with the target molecule,[18] which was in turn dependent on E_{coll} and on the isotopic mass combination of ion and molecule. In this respect, slower collisions would allow a more efficient trapping and randomization of the energy in the complex.[52,53] It is also expected that heavier projectiles will cause a more efficient energy transfer favouring complex formation. Continuing work by many groups has led during the last decade to the construction of precise H_3^+ potential surfaces and to the application of refined statistical models and dynamical treatments to the study of the $H^+ + H_2$ system.[25–43,54–60] Quantum mechanical (QM) reaction probabilities for $D^+ + H_2$ calculated for zero total angular momentum ($J = 0$) led to a good agreement with statistical results,[25,28] but the extension of the QM calculations to values of J other than zero and to the $H^+ + H_2$ and $H^+ + D_2$ isotopic variants[30,40,42,43] confirmed the dynamical bias limiting the validity of purely statistical treatments already advanced in the pioneering studies of the 70s and 80s. This situation encourages a deeper investigation of the dynamics of this reaction with rigorous QM methods, but the extension of precise QM calculations to high E_{coll} and J values remains a challenge to date.

In view of the difficulties for the unrestricted application of accurate QM methods to the $H^+ + H_2$ proton exchange reaction, it is interesting to explore in some depth the merits and shortcomings of alternative treatments. Besides the practical advantages that can be gained by establishing the conditions of validity of the more flexible and computationally much less demanding approximate treatments, the comparison of the different theoretical approaches should provide valuable dynamical insights. In a recent work[43] we have calculated reaction probabilities and cross sections for the $H^+ + D_2 \rightarrow HD + D^+$ reaction using a close coupling (CC) wave packet (WP) quantum mechanical method as well as quasiclassical trajectories and a statistical quasiclassical (SQCT) model. This reaction is endoergic by about 40 meV and this energetic threshold has a crucial influence in the kinetics especially at low temperatures. The WP-QM calculations included angular momenta up to $J = 50$, which ensured a convergence in cross sections for E_{coll} lower than 0.6 eV. The QCT and SQCT calculations were carried out for collision energies from zero to 1.3 eV. Statistical and QCT methods had been shown to perform well in general for the description of the reaction dynamics of H_2 molecules with atoms in excited electronic states, $O(^1D)$, $N(^2D)$, $C(^1D)$ or $S(^1D)$ (see for instance ref. 61–63 and the references therein). The ground-state PESs of these reactions are also largely attractive with deep wells sustaining triatomic complexes. However, appreciable discrepancies between the QM, SQCT and QCT methods were found when applied to the $H^+ + D_2$ reaction.[43] In comparison with the CC QM results, the SQCT calculations, which neglect the dynamics once the centrifugal barrier has been surpassed, tend to overestimate reactivity. In contrast, the QCT results yield too low reaction probabilities and cross sections at high enough total angular momenta and/or collision energies. In addition, the QCT method cannot account properly for the dynamics in the vicinity of the threshold due to the neglect of the zero point energy (ZPE) inherent to the method. In this article we extend the comparison of QM, QCT and SQCT theoretical approaches to the $D^+ + H_2$ isotopic variant of the reaction, which is an important HD source in interstellar space.[64–66] In contrast with the previous case, this reaction is exoergic and thus has no threshold. In addition, simple arguments based on impulsive energy transfer[18] suggest that the mass combination of $D^+ + H_2$ is more favourable for complex formation than that of $H^+ + D_2$ and is expected to present a more "statistical" dynamics.

The article is organized as follows: the theoretical methods and the details of their application are described in section II. Section III contains the CC QM, QCT and SQCT excitation functions, reaction probabilities and products' state distributions together with a discussion in which the various theoretical approaches are assessed and the dynamical characteristics of the title reaction are compared with those of its $H^+ + D_2$ counterpart. The main conclusions from this study are then summarized in section IV.

II. Theoretical methods

A Time-independent QM method

For the $D^+ + H_2$ reaction, the time independent QM results were carried out using the close-coupled hyperspherical method of Skouteris *et al.*[67] on the PES by Aguado *et al.*[27] Results have been obtained for a grid of 382 total energies in the range of 0.275 eV to 0.460 eV (corresponding to a range of E_{coll} between 5 meV and 190 meV for the H_2 $v = 0, j = 0$ state). Tests of convergence were performed by varying the maximum internal energy in any channel, E_{max}, the maximum rotational quantum number j_{max}, and the maximum hyperradius ρ_{max}, trying to minimize the computational time but maintaining the accuracy of the results. Reaction probabilities for $J = 0$ converged to less than a few percent were obtained using a basis set with diatomic energy levels up to $E_{max} = 4.2$ eV and $j_{max} = 60$. The value of ρ_{max} was set at 30 a_0, and 1500 log-derivative propagation sectors were used in the calculations. With these parameters it was found that the resonance structures were reproducible. For $J > 0$ the value of k_{max}, the maximum value of the projection of J and the rotational angular momenta onto the body fixed main axis, was chosen to be the maximum of $\min(J, j)$ and $\min(J, j')$ for each energy. Due to the huge increase of computational cost with the value of k_{max}, the range of calculations was limited to a collision energy $\lesssim$190 meV.

The QM results presented for the $H^+ + D_2$ reaction are the same as those previously reported[43] and correspond to wave packet accurate QM calculations using the DRW code[68,69] on the Kamisaka PES.[28] The details of this calculations can be found in ref. 43.

B Quasi-classical trajectory method

Quasi-classical trajectory (QCT) calculations have been performed for the $D^+ + H_2$ reaction at four collision energies, E_{coll} = 100 meV, 190 meV, 500 meV and 1.0 eV, by running batches of 3×10^5 trajectories at each energy, following the procedures described in refs. 43 and 70. In addition, to determine the energy dependence of the reactive cross section (the excitation function), batches of 2×10^6 trajectories were run by varying the collision energy continuously between 3 meV and 1.6 eV for initial rotational states j = 0–4 following the method described in ref. 71. Additional batches of 5×10^4 trajectories were run between 1 meV and 25 meV to improve the accuracy of the calculations in this range of collision energies.

As for the calculations for the $H^+ + D_2$ isotopic variant, batches of 2×10^5 trajectories were run for initial j = 0–5 in the range of E_{coll} between 5 meV and 1.6 eV. Additional batches of 2×10^5 trajectories were calculated in the low collision energy range for those initial rotational states for which the reaction was exoergic ($j \geq 3$).

The integration step size was chosen to be 4×10^{-17} s. This guarantees a total energy conservation better than one part in 10^4 and conservation of total angular momentum better than one part in 10^6. Due to the long range interaction in the entrance and exit channels, the trajectories were started and finished at an atom–diatom R distance of 10 Å (20 Å at the low range of collision energies).

The rovibrational energies of the diatomic molecules were calculated by semiclassical quantisation of the action using the potential given by the asymptotic diatom limits of the PES and their values were fitted to Dunham expansions in $v + 1/2$ and $j(j + 1)$. The assignment of product quantum numbers was carried out by equating the square of the classical HD molecule rotational angular momentum to $j'(j' + 1)\hbar^2$. With the real value obtained in this way, the vibrational quantum number v' is found by equating the internal energy of the outgoing molecule to a rovibrational Dunham expansion. The usual histogram binning (HB) method consists of rounding the classical (real value) vibrational and rotational quantum numbers to their nearest integers. However, as discussed previously, this rounding procedure may allow the population of states that are energetically closed. In principle, this is not expected to be critical in the case of the $D^+ + H_2$ reaction due to its exoergic character (from the zero point energies of reactants to that of the products). Nevertheless, at low collision energies, as in the case of the endoergic $H^+ + D_2$ reaction, a considerable number of reactive trajectories lead to HD with a vibrational action below its ZPE that, according to the HB procedure, are assigned to v' = 0. As a result, rotational states energetically forbidden are populated.

To overcome this problem, as in previous works,[39,42,43] we have used the Gaussian binning (GB) method,[72,73] whose implementation has been described in detail in ref. 74. Briefly, it consists of weighting each trajectory according to Gaussian functions centred on the correct QM vibrational action in such a way that the closer the vibrational (real value) quantum number of a given trajectory is to the nearest integer, the larger the weighting coefficient is for that trajectory. In the present work, we have used a full-width-half-maximum of 0.1 for the Gaussian functions, but the results are largely insensitive to the precise value of this width. In practice, trajectories whose vibrational action is sufficiently far from the quantal one contribute very little to the total cross section. As a consequence, the ZPE requirement is effectively enforced at the expense of a possible decrease of the reactivity. The comparison of the results obtained by the HB and GB will be presented and discussed in detail in section III.

C Statistical quasi-classical trajectory method

The statistical quasi-classical trajectory (SQCT) method has been detailed in previous publications[36,37,63] and its application to the various isotopic variants of the title reaction has been extensively described.[37,43] In all aspects, the SQCT model is entirely equivalent to its quantal version (SQM),[62] with the sole difference being that trajectories instead of wavefunctions are independently propagated in the exit and entrance channel. It has been thoroughly shown that the agreement between the quantum and quasiclassical statistical approaches is almost perfect (see ref. 36, 37 and 63 for detailed comparisons). The SQCT method uses a discrete sampling (quantisation scheme) of the total, J, and rotational, j, angular momenta, as well as that of the projection of $J(j)$ onto the body fixed axis, k. In contrast to the standard QCT method, trajectories are not integrated until they reach the asymptotic region, but only until they have been captured by the potential well. The capture point is characterised by a sufficiently negative value of the potential energy with respect to the asymptotic limit of the respective arrangement channel. Trajectories that experience this value have certainly surmounted the centrifugal barrier and, in principle, are assumed to be trapped in the potential well.

Capture probabilities must be calculated for all possible arrangement channels and for all the energetically open reactant and product rovibrational and helicity (v, j, k) states at a given total energy. Once the capture probabilities have been determined, reaction probabilities and integral and differential cross section are calculated using the same equations as for the SQM model.[37,62] The SQCT method conserves the triatomic parity, accounts for the diatomic parity, and complies with the principle of detailed balance overcoming the problem of the zero point energy.

The equations that relate the capture probabilities with the various reaction probabilities and cross sections have been presented and discussed in previous works.[36,37,62] We will only recall those concerning the state-to-state reaction probability as a function of the total angular momentum, J, as they will be used hereinafter. The state-to-state reaction probability from the ground rovibrational v = 0, j = 0 reagent's state, $P^J_{v'j'00}(E)$, can be written as:[37]

$$P^J_{v'j'00}(E) = p^J_{000} \times \left[\frac{Q^{J,(-1)^J}_{v',j'}}{D^{J,(-1)^J,e}}\right] \quad (1)$$

where p^J_{000} is the capture probability for the reactant arrangement and (v, j, k) = (0, 0, 0) state and total angular momentum J. The sum over k' of the product's capture probabilities into the product state (v', j') is

$$Q^{J,(-1)^J}_{v'j'} = \sum_{k'=0}^{k_{max}} p^{J,(-1)^J}_{v'j'k'} \quad (2)$$

The denominator of eqn (1) is the sum of the capture probabilities over the open rovibrational and helicity states of the reagents and products:

$$D^{J,(-1)^J,e}_{v'j'} = \sum_{v,j_e} Q^{J,(-1)^J}_{vj_e} + \sum_{v',j'} Q^{J,(-1)^J}_{v'j'} \qquad (3)$$

Notice that the first sum runs over even rotational states to account for the diatomic parity.[42,62] Since $j = 0$ (and thus $k = 0$) has been chosen as an example of initial state, in all these equations only the $I = (-1)^J$ triatomic parity has been considered.[37]

In eqn (1) the p^J_{000} term represents the probability of complex formation from the $v = 0, j = 0$ initial state, whereas the factor within brackets is the probability of breakdown of the complex into the v', j' state of the products. Essential in any statistical model is the implicit assumption that the only requirement for complex formation is the occurrence of the capture. With 'capture' we mean that the centrifugal barrier (or effective barrier if there exists an additional dynamical barrier) is overcome and the system is subject to a negative potential value. Moreover, the statistical model implicitly assumes that once the complex has been formed, *i.e.* the capture has taken place, its lifetime is long enough to allow for the randomization of the energy in the various modes, such that the outcome is purely statistical. Notice, however, that this assumption is not guaranteed since no information is extracted of the dynamics inside the well.

Trajectories for 45 energies were run in the range of 1 meV–1.6 eV collision energies with a closer energy grid below 100 meV. An integration time step of 1.0×10^{-16} s guarantees a total energy conservation better than one part in 10^5 and conservation of total angular momentum better than one part in 10^6. The number of trajectories run was 5×10^4 for the lowest energies and up to half a million for the highest collision energies. The capture potential to determine the complex formation was set at −0.6 eV (see ref. 37 for details)

The QCT and SQCT calculations have been carried out on the PES by Aguado *et al.*[27] In addition, since no comparison is made with experimental results, the nuclear spin statistical weights have not been considered in the results presented here.

III. Results and discussion

Fig. 1 shows the collision energy dependence of the $D^+ + H_2$ ($v = 0, j$) reaction cross section (*i.e.* the excitation function) calculated with the SQCT, QCT-HB and QCT-GB procedures. All the calculated cross sections show a monotonic decrease with E_{coll}, in accordance with the expectations for barrierless, exoergic reactions. Over the energy range considered, the largest cross sections correspond to the SQCT method and the smallest ones to the QCT-GB approach. The QCT-HB calculations yield cross sections in good agreement with those from the statistical procedure for the lower energies, but tend towards the GB result with growing E_{coll}. Beyond 0.6 eV, the GB and HB cross sections are indistinguishable. Increasing the rotational quantum number of the H_2 molecule from $j = 0$ to $j = 4$ produces only small changes in the results of the statistical approach, but has an appreciable influence on the QCT-GB $\sigma_R(E_{coll})$, which grows in the lowest (< 0.2 eV) E_{coll} range as j increases from 0 to 4.

In the low range of E_{coll} and $j \leq 3$, the difference between the QCT-HB and QCT-GB is noticeable. This discrepancy must be due to the quantisation procedure applied in each case since this is the only difference between the two methods. As will be discussed below, trajectories at the lowest E_{coll} mainly proceed *via* the formation of a long-lived complex whose lifetime is long enough to allow the randomization of the energy. In the classical case, the absence of the zero point energy constraint makes possible an unrealistic vibrational distribution peaking at a vibrational action, $v' + 1/2$, equal to zero and thus most of the reactive trajectories lead to HD products whose vibrational content is well below its ZPE. With the GB quantisation method, however, trajectories leading to vibrational energies close to the values of the actual quantum states of HD are much more strongly weighted than the rest; therefore, a very substantial number of reactive trajectories contributes with an almost negligible weight to the total cross section. In contrast, the QCT-HB procedure attributes the same weight to all reactive trajectories irrespective of the proximity of their classical vibrational energy to that of a molecular quantum state and the resulting cross section is much larger than in the QCT-GB case as long as the maximum classical v is low enough. It might be argued that this unbiased trajectory weighting could be more realistic for the estimate of total cross sections in reactions without a threshold like that presently considered. Actually, the coincidence between the cross section obtained with this method and with the SQCT is very good in this low range of collision energies. Nevertheless, as we will see below, the QCT-HB method fails to account for other more resolved dynamical magnitudes and leads to unrealistic results.

With increasing collision energy and, especially, with growing j, the QCT calculations lead to a broader distribution of HD vibrational energies covering a larger range of classical vibrational actions and the $\sigma_R(E_{coll})$ from the two quantisation methods approach gradually. As mentioned above, the SQCT cross sections for collision energies below 0.2–0.3 eV are similar to those given by the QCT-HB procedure, although the former complies with the ZPE restriction. As indicated in former works,[13,52,53] statistical treatments are especially successful for comparatively long collision times that allow for an efficient randomization of the available energy within the reaction complex.

The results commented on in the previous paragraph can now be compared to those obtained for the endoergic $H^+ + D_2$ ($v = 0, j = 0$–4) isotopologue of the same system, which are displayed in Fig. 2. A detailed analysis of the dynamics of the $H^+ + D_2$ ($v = 0, j = 0$) reaction was reported in ref. 43. In that work the calculations were carried out on the potential energy surface by Kamisaka *et al.*[28] and $j = 0$. As indicated in the method section, the calculations of the present study have been performed on the PES by Aguado *et al.*,[27] but, except for some small differences at low collision energies (E_{coll} < 100 meV), the two PESs lead to the same results.[75] In Fig. 2, the presence of a reaction threshold, corresponding to the energy difference between the ground vibrational levels of HD and D_2 is clearly reflected in the shape

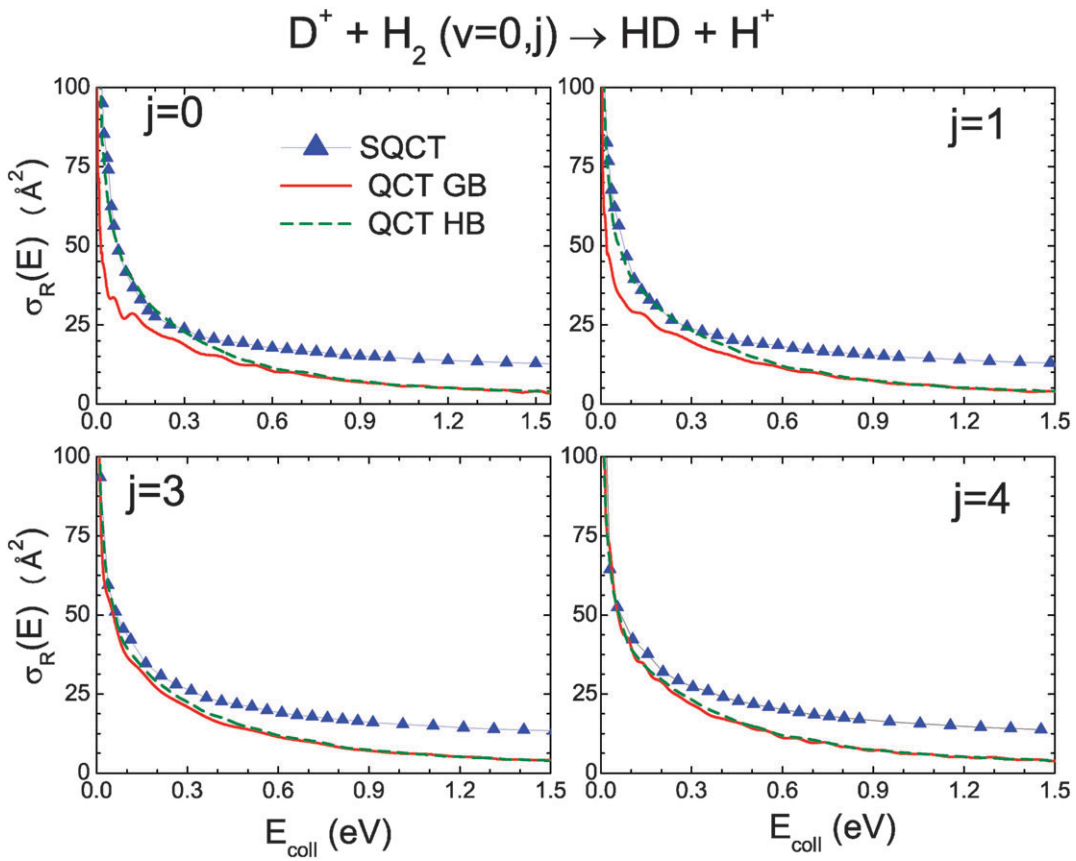

Fig. 1 Excitation functions (collision energy dependence of the reactive integral cross section) for the $D^+ + H_2$ ($v = 0, j$) $\rightarrow H^+ + HD$ reaction for $j = 0$, 1, 3, and 4 initial rotational states. Dash (green) line: QCT-HB results. Solid (red) line: QCT-GB results. Triangles and solid (blue) line: SQCT results. The nuclear spin statistics has been disregarded.

of the SQCT and QCT-GB excitation functions for $j = 0$ (upper left panel). As expected, the reaction threshold coincides with the difference of the zero point energies, $\approx$42 meV, and beyond the threshold, the cross section rises sharply and reaches a maximum located at 125 meV for the statistical method and at 200 meV in the QCT-GB calculations. Above the energy of the maximum the two methods predict a smooth decrease in the value of the cross section. The QCT-HB results show only a monotonic decline of the cross section with collision energy. As already mentioned, this method cannot account for the existence of this kind of threshold since it unbiasedly includes all trajectories leading to reaction irrespective of their final vibrational energy, which can be well below that of the HD ground vibrational state. For collision energies larger than 0.35 eV the same QCT cross sections are obtained with the two quantisation procedures. Except for the QCT-HB method at the lowest E_{coll}, where the neglect of the threshold leads to artificially high values of the cross sections, the SQCT $\sigma_R(E_{coll})$ is always larger than those from QCT calculations and the difference increases with growing collision energy. The fact that the SQCT model gives rise to cross sections remarkably larger than those found in QCT calculations is a common feature for the two reactions studied in this work (see also Fig. 1). This effect suggests that as the collision energy increases the QCT behaviour departs from a purely statistical mechanism and genuine dynamical effects take place. As will be discussed below, higher energies imply that more trajectories are direct, spending a short time in the well, and, moreover, do not lead to HD formation in the ratio expected according to statistical arguments.

When the D_2 molecules have one quantum of rotational excitation (upper right panel), the threshold is still present in the SQCT and QCT-GB calculations and the various excitation functions have shapes that do not differ much from those just discussed for $j = 0$. However, for $j = 3$ (lower left panel) the reaction is already slightly exoergic (1.89 meV) and the threshold disappears in all cases. In spite of having no threshold, the SQCT and QCT-GB excitation functions still show maxima for this nearly thermoneutral condition. For $j = 4$ (lower right panel), with a higher exoergicity, the remnants of the maxima are practically absent and the three σ_R exhibit essentially a decline with E_{coll}, a behaviour that is qualitatively similar to that found for $D^+ + H_2$ over the whole range of energies and j values considered. Notice that the good accordance between the HB and GB excitation functions starts at lower energies as the initial D_2 rotational states increase, similar to what was observed for the $D^+ + H_2$ reaction. For all the rotational levels, the differences between the QCT and SQCT cross sections at high energies are somewhat larger for the $H^+ + D_2$ reaction. From the comparison of the respective excitation functions of the two isotopic variants, it seems that this mass combination is less effective than $D^+ + H_2$ for the

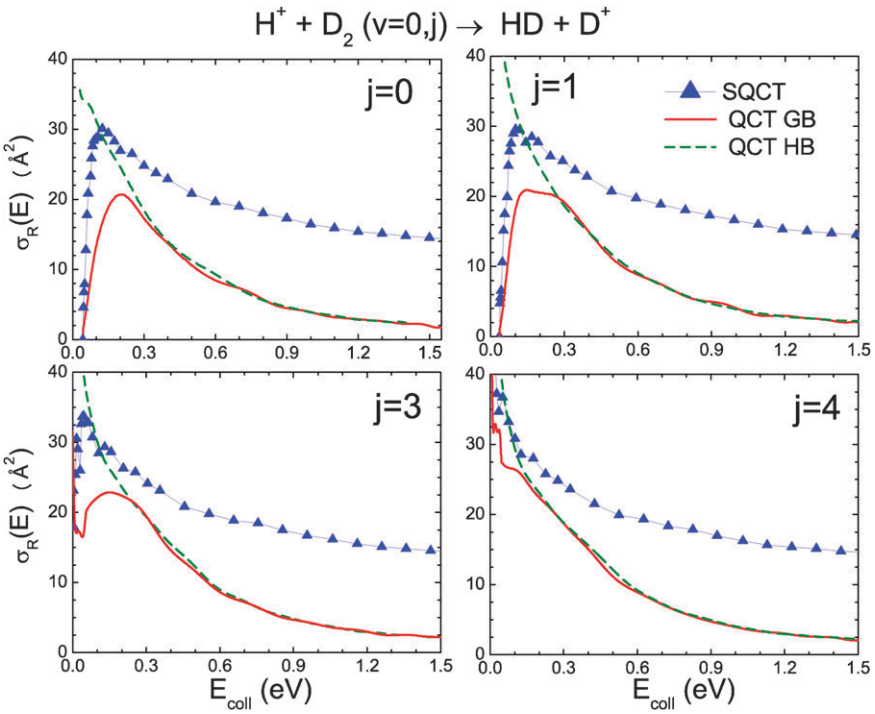

Fig. 2 Same as Fig. 1 but for the $H^+ + D_2$ ($v = 0, j$) $\rightarrow D^+ + HD$ reaction. As in Fig. 1, the nuclear spin statistics have been disregarded.

transfer of the initial ion energy to the molecule and thus for the trapping of the reactants into a long-lived complex, and, therefore, it is expected to deviate more from the statistical behaviour, as pointed out by Schlier and Vix.[18]

In our previous work[43] the limitations of QCT and SQCT methods for the description of the $H^+ + D_2$ reaction dynamics were demonstrated in a thorough comparison with accurate quantum mechanical calculations. The comparison between accurate QM, SQCT, and QCT reaction cross sections is extended to the $D^+ + H_2$ system in the top panel of Fig. 3. Accurate QM results have been obtained with the time independent method described in the previous section and are limited to total energies below 460 meV ($E_{coll} < 200$ meV for H_2 in $v = 0$, $j = 0$) due to the inherent difficulties mentioned above. In spite of the restricted energy and internal state range, these calculations cover, to a large extent, the conditions prevailing in the interstellar medium, where this reaction is particularly relevant. Overall, the best agreement with the QM results is obtained with the QCT-HB method. Below 50 meV, the cross sections calculated with this method lie within the oscillations of the QM resonance structure. For higher E_{coll} values, the QCT-HB cross sections become slightly larger that their QM counterparts. The SQCT calculations also perform reasonably well, although they yield cross sections which are somewhat higher than those from quantum mechanics over the whole interval considered. In contrast with the other two methods, the QCT-GB procedure leads to cross section values which are markedly lower than those from the QM calculations in the lowest energy range considered. Only for collision energies larger than 100 meV do the QCT-GB cross sections get close to the quantum mechanical values.

The bottom panel of Fig. 3 displays the SQCT, QCT (HB and GB) and QM excitation functions for $H^+ + D_2$

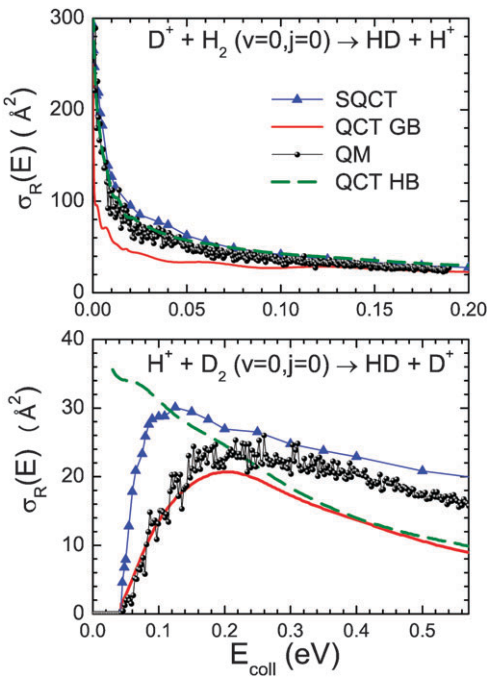

Fig. 3 Excitation functions for the $D^+ + H_2$ ($v = 0$, $j = 0$) $\rightarrow$ $H^+ + HD$ (top) and $H^+ + D_2$ ($v = 0, j = 0$) $\rightarrow D^+ + HD$ (bottom) reactions in the low collision energy range. Filled circles and solid line: QM results. Dash (green) line: QCT-HB results. Solid (red) line: QCT-GB results. Triangles and solid (blue) line: SQCT results. The WP-QM data for the latter reaction are from ref. 43.

over the 0–0.6 eV collision energy range. The accurate QM results have been taken from ref. 43 and correspond to wavepacket calculations on the PES by Kamisaka *et al.*[28] but, as mentioned above, the differences between dynamical

calculations on that surface and those on the PES by Aguado *et al*., used in this work, are small and irrelevant for the present discussion.[75] A comparison of the two panels of Fig. 3 reveals that, whereas for $H^+ + D_2$ the agreement between accurate QM and QCT-GB is fairly good at collision energies below 200 meV, for the $D^+ + H_2$ (top panel) this binning procedure underestimates the reactivity for $E_{coll} < 100$ meV. In contrast, the standard QCT-HB method that describes the low energy region of the $\sigma_R(E_{coll})$ for the latter reaction fails in the prediction of the threshold and post-threshold behaviour of the $H^+ + D_2$. This is not altogether surprising, since, as commented on above, the existence of a ZPE threshold is directly ignored in the HB method, which is thus unsuitable for $H^+ + D_2$. On the other hand, for the exoergic $D^+ + H_2$ reaction, a substantial fraction of reactivity at the lowest energies is underestimated in the GB scheme which consequently yields too low cross sections. For both reactions, the SQCT method leads to the highest cross sections. The deviation of the statistical calculations from those obtained with dynamical procedures and especially from the accurate QM results suggests that the reactivity is dynamically biased to some extent even at low collision energies. In the case of $H^+ + D_2$, where the QM calculations extend to 0.6 eV, the QCT cross sections become appreciably smaller than their quantum mechanical counterparts for collision energies larger than approximately 0.25 eV, indicating that dynamical constraints are probably overestimated in the classical mechanics calculation. By analogy with this system, it could be conjectured that in the case of $D^+ + H_2$, the QM cross section for $E_{coll} > 0.3$ eV would take values between those from the QCT and SQCT approaches, possibly closer to the SQCT result, given the presumed higher statistical character of the $D^+ + H_2$ kinetics, but further calculations are needed to verify this conjecture.

The failure of the QCT-GB method to account for the accurate QM excitation function for the $D^+ + H_2$ reaction and the seemingly good agreement obtained with the HB procedure encourages the extension of this comparison to a higher level of detail by considering more specific dynamical observables. Fig. 4 displays the opacity functions, *i.e*. the reaction probabilities *vs*. total angular momentum, $P_R(J)$, for the $D^+ + H_2$ ($v = 0, j = 0$) reaction at four collision energies. The two upper panels, corresponding to collision energies of 100 and 190 meV, include results from accurate QM calculations. For the higher E_{coll} values (lower panels), the comparison is restricted to the SQCT and QCT methods.

At $E_{coll} = 100$ meV, the QM opacity function displays a resonance structure characterized by very strong oscillations in the $P_R(J)$ values. The three approaches that account for the ZPE conservation predict a null reactivity for $J > 30$, whilst for the QCT-HB calculations it extends to $J = 31$. The QCT-HB and SQCT calculations for this energy lead to similar results: the $P_R(J)$ lies between 0.7 and 0.8 from $J = 0$ to $J = 29$ and then decreases abruptly. In the QCT-HB opacity function, most of the decline takes place between $J = 30$ and $J = 31$. The QM opacity function also shows a steep decline above $J = 27$. The QM results are on average somewhat lower than those from SQCT and QCT-HB. In contrast to the other methods, the QCT-GB opacity function shows a smoother decline with growing J, starting at $J = 5$ and becoming more pronounced after $J = 15$. Below $J = 15$, the QCT-GB leads to the best agreement with the average value of the accurate QM reaction probability; beyond this J value, the QCT-GB $P_R(J)$ are lower than those from the other methods. At $E_{coll} = 190$ meV (upper right panel), apart from a larger value of J_{max}, the maximum value of the total angular momentum leading to reaction, the general pattern of the opacity functions calculated with the various methods, is analogous to that at $E_{coll} = 100$ meV. The QCT and SQCT $P_R(J)$ take at first a nearly constant value of approximately 0.7, and the QM opacity function oscillates around this value, although the oscillations are less marked than for $E_{coll} = 100$ meV. Beyond $J = 20$, the results of the various approaches diverge. Again in this case the reactivity extends to larger J values in the QCT-HB calculations with a $J_{max} = 37$, whereas the rest of the $P_R(J)$ are zero for $J > 35$. The two QCT $P_R(J)$ initiate a gentle decline at about $J = 20$ and then descend abruptly when approaching their respective J_{max} values. At this energy, the overall best agreement with the QM calculations is obtained with the SQCT method, although the two QCT approaches also perform reasonably well.

It should be noted here that the agreement between opacity functions from SQCT and QM is better for this isotopic variant than for $H^+ + D_2$ (see Fig. 7 and 8 of ref. 43), again in accordance with the higher likelihood for complex formation expected for $D^+ + H_2$.[18] With increasing collision energy (two lower panels of Fig. 4) higher J_{max} values are reached. At these higher energies, the SQCT opacity functions are fairly constant until their final sudden fall. In contrast, the QCT $P_R(J)$ start declining at comparatively low J values; the decline becoming steeper as J_{max} is approached. At $E_{coll} = 500$ meV, the SQCT and QCT-GB opacity functions have a $J_{max} = 49$ whereas the QCT-HB $P_R(J)$ extends to $J_{max} = 51$, albeit with a low probability. At $E_{coll} = 1.0$ eV the QCT reaction probability is zero for $J > 51$, a value much lower than the $J_{max} = 61$ found in the SQCT calculations. The faster decrease in the QCT reaction probabilities at high energies, especially for the higher J, in comparison with the SQCT results, is similar to that found for the $H^+ + D_2$ reaction. The fact that the SQCT reaction probabilities, and thus cross sections, are much larger than the QCT ones rules out any phenomenon associated with the centrifugal barrier in the entrance channel. The decrease of the QCT reactivity is due to trajectories that have surmounted the centrifugal barrier but, nevertheless, experience a short range centrifugal repulsion, inside the triatomic well of the potential surface turning them back to the reactant channel. This dynamical restriction is obviously absent in the SQCT model, where the reaction probability is determined by capture probabilities based on the ability of surmounting the centrifugal barrier located outside the triatomic potential well. Although QM opacity functions are not yet available at these collision energies, they would possibly lie between those from the QCT and SQCT methods, in analogy with the results obtained for the $H^+ + D_2$ isotopic variant and the opacity functions at lower collision energies.

In order to further understand some of the features of the opacity functions presented in Fig. 4 and, in particular, the connection of the maximum value of J and the ZPE

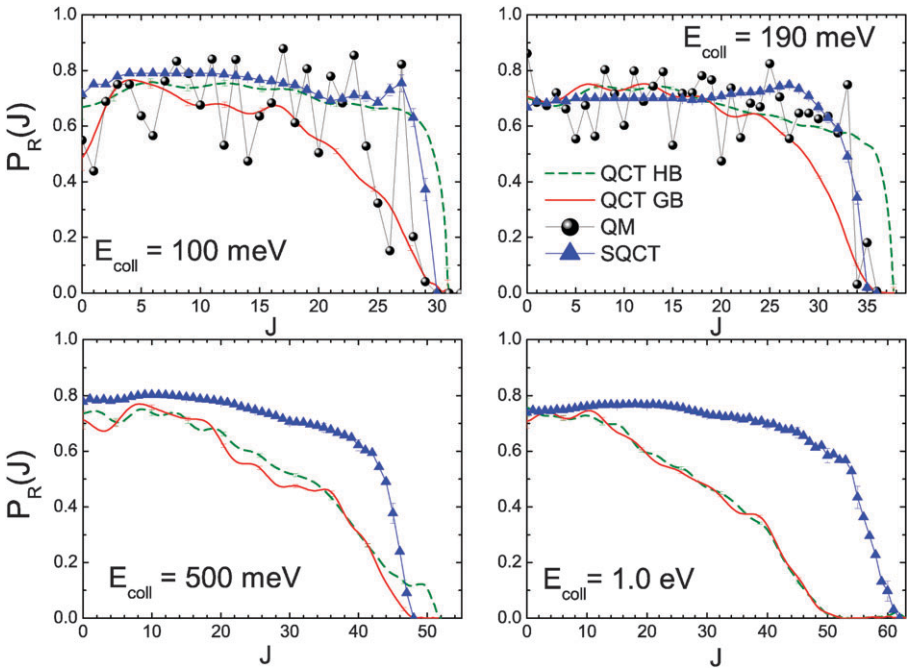

Fig. 4 Opacity function for the $D^+ + H_2$ ($v = 0, j = 0$) reaction summed over final states at E_{coll} = 100 meV, 190 meV, 500 meV and 1.00 eV. Dash (green) line: QCT-HB results. Solid (red) line: QCT-GB results. Triangles and solid (blue) line: SQCT results. Filled circles and solid line: QM results (two upper panels).

compliance, it is pertinent to determine the opacity functions for the $D^+ + H_2$ reaction resolved into the rotational states of the HD($v' = 0$) product molecule. Fig. 5 depicts the j' resolved opacity functions at E_{coll} = 190 meV for $j' = 0$–5. As will be shown below, $j' = 5$ is the maximum value energetically accessible. The choice of this energy stems from the fact that the difference between the J_{max} values obtained in the QCT-HB and the rest of the approaches is noticeable and it can be expected to be related to the problem of the products' zero point energy. Additionally, at this collision energy the agreement between QM and the prediction of the statistical models seems to be quite good. As can be seen, the QM $P_{v'=0j'}(J)$ exhibits pronounced oscillations in all cases that persist once the summation over j' is carried out (see the upper right panel of Fig. 4). Comparing the QM results with those obtained with the SQCT and the two QCT procedures and leaving aside the oscillations, it is evident that the best agreement is obtained between the QM and the SQCT results. The QCT calculations yield too low probabilities for the lowest rotational state, but with increasing j' the agreement between QM (and SQCT) and QCT-GB becomes much better. The QCT-HB method produces the worst accordance with the QM results over the whole range of j' displayed in the figure. The reaction probabilities for individual j' values are lower and reach higher J_{max} values than those from the other sets of calculations. This effect is especially conspicuous for $j' \geq 3$ and connects with the finding that in the total opacity function the QCT-HB reaches the largest J_{max} values at this collision energy. Except for the QCT-HB opacity functions, where J_{max} does not change over the j' range considered, there is a negative correlation between J_{max} and j'. For this isotopic variant the value of J_{max} is limited by the exit channel. For a given total energy and a fixed value of the HD vibrational energy, as j' increases the available translational energy to surmount the centrifugal barrier decreases and, as a result of this, the largest J allowed diminishes. This is exactly what is observed in the three sets of calculations that comply with the zero point energy constraint. However, in the QCT-HB method there is no limitation to the minimum value of the vibrational energy, and consequently the translational energy necessary to overcome the barrier can be drawn from and at the expense of the vibrational excitation.

In addition, it is not surprising that the reaction probability for intermediate J values ($J \leq 20$) increases with the product rotational excitation since the number of projections k' of the total (and HD rotational) angular momentum that contribute to the reaction rises with j'. Similar arguments, drawn from the SQCT model, serve to explain the maxima that can be observed near the values of J_{max}, especially for $j' \leq 3$. As can be derived from eqn (1), the J-dependent denominator of the expression of the $P^J_{0j',00}$, eqn (3), is nearly constant up to $J = 18$, since all the possible (v, j, k) energetically open channels of reagents and products are accessible. With growing J, the centrifugal barrier causes the closing of exit channels corresponding to the highest rotational HD levels (see the lower panels of Fig. 5) and, consequently, the denominator decreases. As a result, the reaction probability for the lower j' states grows for values of J beyond $\approx$18 and gives rise to a maximum in the reaction probability in the vicinity of their respective J_{max}.

Notice that differences observed with j' are due to changes in the probability of the breakdown of the complex into the various final states rather than to the probability of complex formation (see eqn (1) and section II). The fact that all the

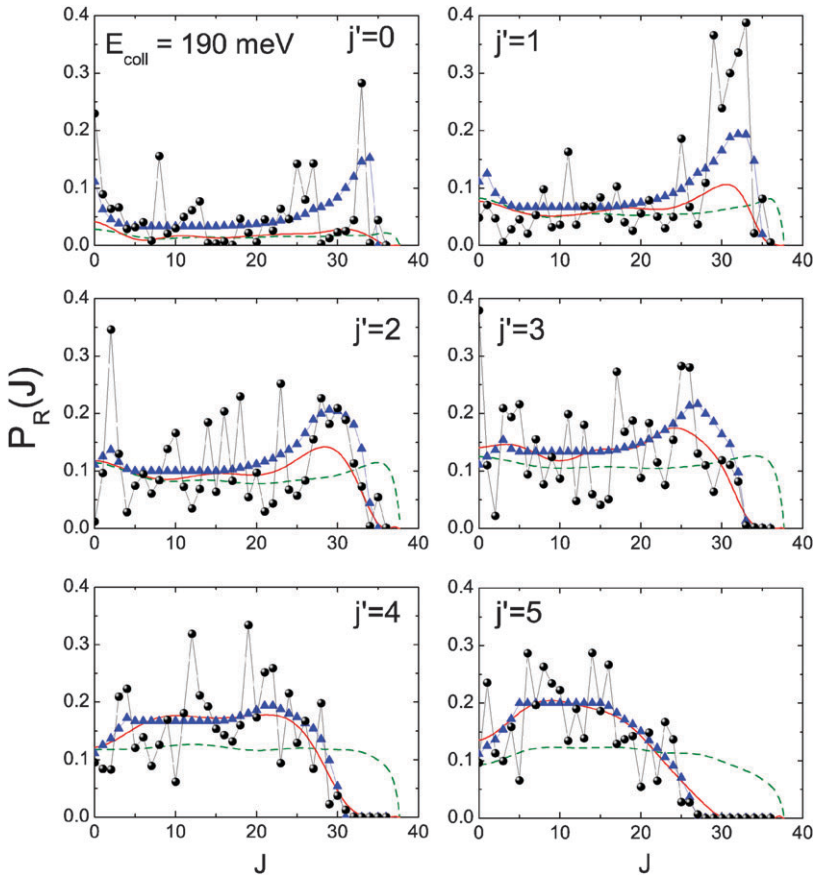

Fig. 5 Opacity function for the $D^+ + H_2$ ($v = 0, j = 0$) → $H^+ + HD$ ($v' = 0, j'$) reaction at $E_{coll} = 190$ meV. Dash (green) line: QCT-HB results. Solid (red) line: QCT-GB results. Triangles and solid (blue) line: SQCT results. Filled circles and solid line: QM results (see text for details).

features observed, except for the oscillation due to the underlying resonance structure, can be explained with the statistical model underpins the statistical character of the reaction in this range of collision energies between 0.1 and 0.3 eV.

Fig. 5 includes reaction probabilities for all the j' values that are energetically open in the QM and SQCT calculations at $E_{coll} = 190$ meV. A comparison of Fig. 4 and 5 shows that an appreciable amount of the QCT-HB reactive flux must be channelled into other rotational levels of HD. This is best seen in Fig. 6, where the $v' = 0$ integral cross sections for the production of the different rotational levels are represented. As in the previous cases, QM calculations are restricted to $E_{coll} < 200$ meV. For 100 meV and 190 meV collision energies the rotational distributions of HD calculated with the QCT-HB method are appreciably broader than the rest and extend to $j' = 8$ and 9, respectively, whereas the value of j'_{max} allowed by energy conservation is three to four quanta lower. Both the higher J_{max} of Fig. 5 and the higher j'_{max} of Fig. 6, derived with the QCT-HB method, are essentially due to the neglect of the ZPE of the HD molecule commented on in the previous paragraphs. Within this approach the system, whose vibrational energy can go to zero, is allowed to reach a higher rotational energy for a given E_{coll}. The QCT-GB calculations reproduce well the higher j' range of the QM distributions including their final decline, but the calculated cross sections are too small for the lower j' values. Overall, the best agreement with QM is obtained with the SQCT procedure, but some discrepancies are also found around the maximum.

For the two higher energies (lower panels of Fig. 6), appreciable differences are found between the QCT and SQCT rotational distributions in $v' = 0$. The discrepancy is especially large in the lowest j' states, where the statistical approach, unaffected by the dynamical bias associated with fast collisions, leads to much higher cross sections, especially at $E_{coll} = 1.0$ eV. As can be seen, the SQCT calculations favour low rotational states whilst the opposite is true with the QCT results. As a result of this, the shapes of the SQCT and QCT rotational distributions are clearly different. At these collision energies, the QCT-HB $v' = 0$ rotational distribution is nearly identical to that obtained with the GB procedure, and the effect of that binning on the global reactivity is very small for collision energies much larger than that of the zero point energy of HD.

The evolution of the distribution of available energy between the various modes of the reaction products as a function of E_{coll} is shown in Fig. 7. The average fractions of translational, $\langle f_T \rangle$, rotational, $\langle f_R \rangle$, and vibrational, $\langle f_V \rangle$, energy calculated with the QM, SQCT and QCT-GB methods are represented in this figure for the $D^+ + H_2(v = 0, j = 0)$ (upper panel) and $H^+ + D_2(v = 0, j = 0)$ (lower panel) reactions. Note the overall similarity in the results for the two systems. Immediately after the reaction threshold in the case of

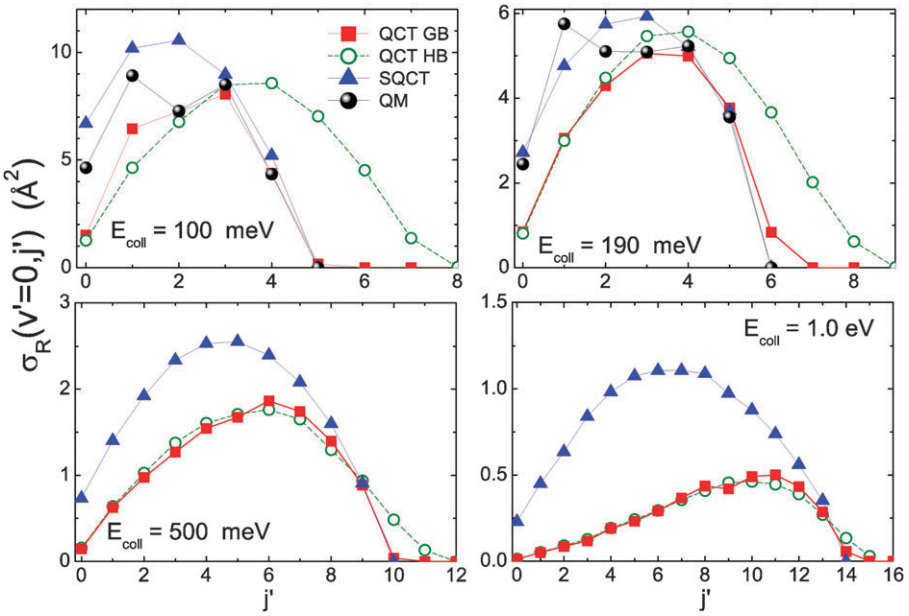

Fig. 6 Integral cross section for the $D^+ + H_2$ ($v = 0, j = 0$) → $H^+ + HD$ ($v' = 0, j'$) reaction at E_{coll} = 100 meV, 190 meV, 500 meV, and 1.0 eV. Open (green) circles and dashed line: QCT-HB results. Squares and solid (red) line: QCT-GB results. Triangles and solid (blue) line: SQCT results. Filled circles and solid line: QM results.

$H^+ + D_2$, or after the E_{coll} origin for $D^+ + H_2$, the products' energy is mostly concentrated as vibration in the ground state of HD, as required by the ZPE constraint; with increasing E_{coll} more energy becomes gradually available for translational and rotational motion and $\langle f_V \rangle$ decreases steadily as $\langle f_T \rangle$ and $\langle f_R \rangle$ grow. At about 0.3–0.4 eV, $\langle f_T \rangle$ becomes the largest fraction and for higher collision energies the various energetic fractions remain roughly constant in the SQCT calculations, with $\langle f_V \rangle$ and $\langle f_R \rangle$ (in that order) taking smaller and not too different values. Note that in the high energy range (above 0.6 eV), far from the energetic restrictions of the post threshold region, the SQCT calculations predict a higher fraction of products' translational energy (and thus a lower proportion of internal energy) for $D^+ + H_2$ where it takes a value of 0.5 as compared to 0.4 for $H^+ + D_2$.

In the QCT-GB calculations the fractions of available energy in internal and translational degrees of freedom tend to practically the same value of ≈0.33 at $E_{coll} > 0.8$ eV for the HD_2^+ system and to somewhat higher energies for the $D^+ + H_2$ reaction. The results of the QCT-HB calculations, not represented for clarity, have no constraints associated with the vibrational threshold and the respective $\langle f_T \rangle$, $\langle f_R \rangle$ and $\langle f_V \rangle$ values are only comparable with the QCT-GB results for $E_{coll} \geq 0.6$ eV. The QCT-GB energetic fractions are in reasonable agreement with the accurate QM predictions available at low collision energy, but the accordance is better between QM and SQCT results.

In the high energy range, it is interesting the difference in the fractions obtained by the QCT and SQCT methods that should reflect the dynamical bias that has been found in other dynamical quantities using the former approach. The actual statistical limit obviously corresponds to the SQCT results. The statistical model can be further simplified by assuming: (a) that the capture probabilities from all energetically accessible states of the reagents and products are equal to one, and (b) that the limiting J_{max} value at a given energy only depends on each particular rovibrational state of the products. For the $D^+ + H_2$ reaction, the J_{max} value is limited by the exit channel, $HD + H^+$, whose capture probabilities die out sooner than those from the $D^+ + H_2(v = 0, j = 0)$ channel. The actual dependence of J_{max} on the (v', j') state is basically given by the simple centrifugal barrier model, approximately leading to $J_{max} \propto E_T'^{1/2}$, where E_T' is the available energy in translation for a given (v', j') HD state. With this simplification the resulting $\langle f_T \rangle$, $\langle f_R \rangle$ and $\langle f_V \rangle$ have values very close to those given by the rigorous SQCT model, especially in the high energy range. Note that within the SQCT model, 50% of the available energy is released as translational energy; that is, roughly speaking, the total energy is equally partitioned among the various degrees of freedom. For the $H^+ + D_2$ reaction the model needs some refinement since the J_{max} value can be limited by either the $H^+ + D_2(v = 0, j = 0)$ or the various product's $D^+ + HD(v', j')$ channels. In the end, the agreement with the rigorous SQCT model is also good. Notice that the SQCT model predicts for this reaction a $\langle f_T \rangle \approx 0.4$, slightly lower than that obtained for the other isotopic variant.

The $\langle f_i \rangle$ values in the different degrees of freedom obtained from the QCT-GB can be also reproduced using a biased statistical model wherein the J_{max} value has to be enforced and is smaller than that deduced by simple centrifugal barrier arguments. Using a limiting value of $J_{max} \approx 50$ (see Fig. 4), the results are very similar to those shown in Fig. 7. In the QCT limit, at sufficiently high collision energies, approximately 1/3 of the total energy is allocated in each mode. The substantial difference in the SQCT and QCT predictions of the energy disposal in translational and internal degrees of freedom is a reflection of the dynamical bias found in the QCT results. The accessibility of considerably higher values of J in

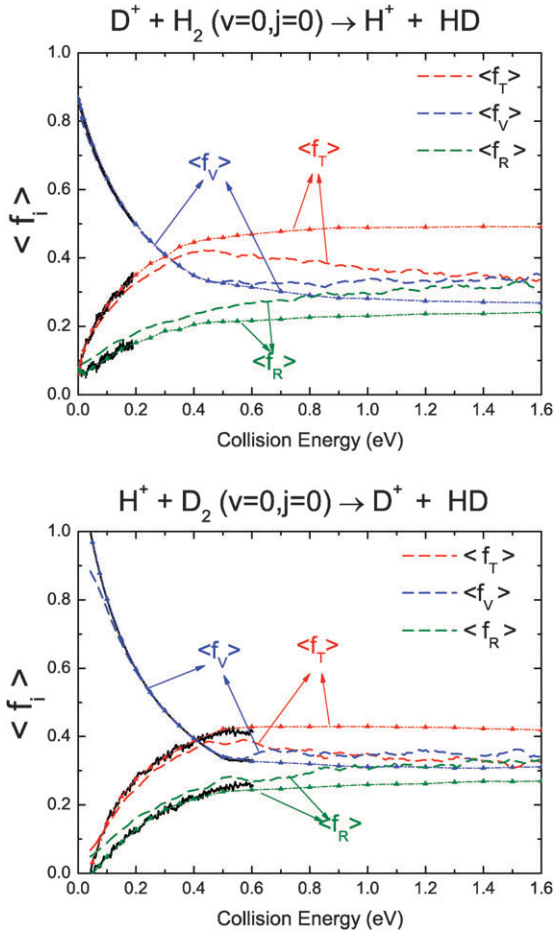

Fig. 7 Average fraction of the available energy into translation, rotation and vibration of the products as a function of the collision energy for the $D^+ + H_2$ reaction (top panel) and the $H^+ + D_2$ reaction (bottom panel) calculated with QM (solid line), QCT-GB (dashed line), and SQCT (dash-dotted line and triangles) methods.

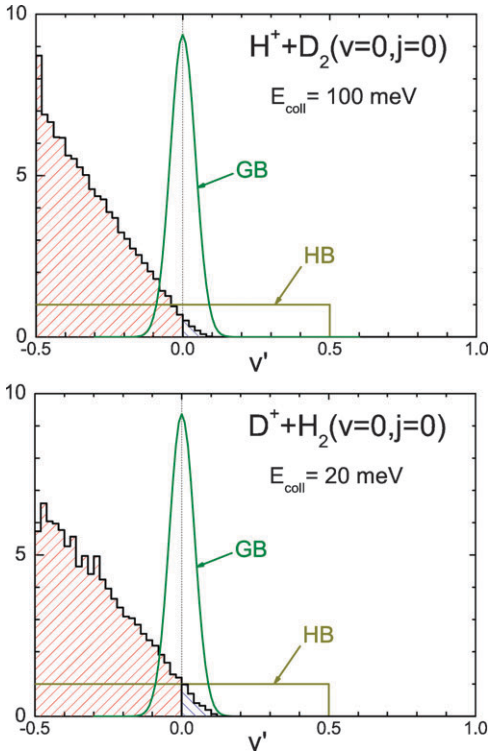

Fig. 8 Classical vibrational distribution for the HD molecule from the $H^+ + D_2$ (top) and $D^+ + H_2$ (bottom) reactions at 20 meV and 100 meV collision energy, respectively, such that the total energy is practically the same. The weighting functions for the normal histogram and Gaussian binning procedures are also shown and serve to illustrate the differences between the two final state assignments.

the SQCT calculations (see Fig. 4 and ref. 43) leads to the predominant formation of HD products in low rotational states of the $v' = 0$ manifold. In contrast, the drastic limitation of the J_{max} values found in the QCT calculations reduces the population of low j' states. The net effect is that a smaller fraction of the available energy appears as translation in the QCT calculations.

A closer inspection of the two panels of Fig. 7 shows that a very good match between the $\langle f_T \rangle$, $\langle f_R \rangle$ and $\langle f_V \rangle$ curves of the two reactions can be achieved in the low E_{coll} range if the collision energy scale is shifted by about 80 meV, which corresponds to the difference between the exoergicities of the two reactions. When the E_{coll} of the $H^+ + D_2$ reaction (endoergic by about 40 meV) is 80 meV larger than that of $D^+ + H_2$ (exoergic by 40 meV), the amount of energy available to the products is the same for the two systems and this energy is distributed in a similar way among the various degrees of freedom in both reactions.

This point is further illustrated in Fig. 8, which shows the similar QCT vibrational energy distributions of the HD molecules produced in the $D^+ + H_2$ and $H^+ + D_2$ reactions at $E_{coll} = 20$ meV and 100 meV, respectively. In both cases the same amount of energy ($\approx$60 meV) is available to the products. The abscissa scale in this figure corresponds to the classical (real value) vibrational quantum number and its zero is located at the HD($v' = 0$) vibrational level. As can be seen, the classical (continuous) vibrational distributions are very similar in both cases, with maxima at $v' = -0.5$ and declining rapidly with v', such that only a small fraction of the HD molecules are produced in or around $v' = 0$. The two QCT binning procedures used throughout the article are also sketched in the figure. In the HB scheme, a weight of one is assigned to each reactive trajectory regardless of the proximity of its vibrational quantum number to the quantum (integer) value. The weight function is thus a step function of unit height spanning a unit of vibrational number. In the two cases shown in Fig. 8, the step function extends from $v' = -0.5$ to $v' = 0.5$, *i.e.* a weight of one is assigned to each reactive trajectory, which is equivalent to round their respective real value vibrational quantum number to zero. In the GB method reactive trajectories are weighted with normalised Gaussian distributions, each of them centred at the successive integer vibrational quantum number. For the case under consideration, the Gaussian function is centred at $v' = 0$ and has a FWHM of 0.1 (see ref. 43 for more details).

Fig. 8 clearly shows that for both isotopic variants at the low E_{coll} values considered here most of the reactive trajectories lead to vibrational quantum numbers well below the ZPE of the HD molecule. This result is not surprising in a

classical treatment of a statistical reaction. At a sufficiently low total energy, the collision time is long enough to randomise the energy channeled into the various modes. Therefore, in the absence of ZPE constraints, the product vibrational distribution is expected to peak at zero vibrational energy ($v' = -0.5$) and decay monotonically with v'. As a consequence, the energy disposal in rotation is overestimated, leading to anomalous rotational distributions and, in the case of the endoergic $H^+ + D_2$ reaction, the method predicts a high reactivity below the reaction thermochemical threshold. The application of the GB procedure, which assigns negligible weights to those trajectories with a vibrational energy content much lower than that of $v' = 0$, eliminates effectively the majority of trajectories below the ZPE. Note that the cross section is the integral of the product of the classical vibrational distribution and the normalized Gaussian distribution, whereas for the standard HB, it is just proportional to the integral of the vibrational distribution since the weights are always one. With these considerations, it is relatively simple to determine under what circumstances the cross section will be the same with the two procedures, being essentially dependent on the energy available to the products (proceeding either from translational or rotational energy of the reactants), and consequently, the maximum v' classically allowed, v'_{max}. A simple model approximating the vibrational distribution to a linear dependence with v' can show that for $v'_{max} \approx 0.5$ the cross section produced by the two procedures will be almost the same. Therefore, for energies available to the products above a certain value and, as long as the classical vibrational distribution is statistical (decaying monotonically with v'), the GB procedure will not introduce any bias in the reaction cross section.

IV. Summary and conclusions

Three theoretical approaches, namely, close-coupling QM calculations, quasiclassical trajectories, and a statistical quasiclassical trajectory method, have been tried for the investigation of the dynamics of the $D^+ + H_2 \rightarrow HD + H^+$ reaction. This system is not only a prototype for dynamical studies of ion-molecule reactions, but also an important source of HD in interstellar space, where it plays a decisive role in the observed deuterium fractionation. Reaction probabilities, cross sections, and products' state distributions have been calculated on the adiabatic ground state PES potential surface of the H_3^+ system. The accurate QM calculations are difficult and computationally expensive due to the presence of a deep potential energy well corresponding to the formation of the DH_2^+ complex and have only been performed for collision energies below 0.2 eV. Approximate methods are then used to study the dynamics over an extended range of collision energies ($E_{coll} = 0$–1.3 eV) and rotational states ($j = 0$–4) of H_2. In the quasiclassical calculations, two schemes have been used for the binning of trajectories: the standard histogram binning (HB), in which all reactive trajectories have the same weight, and the Gaussian binning (GB), in which a larger weight is given to trajectories in the vicinity of an actual quantum state of the HD product molecule. Although the comparison with the accurate QM results shows that the agreement with the QCT-HB procedure is better for the calculation of the total cross section in this barrierless exoergic reaction, the method fails for the calculation of more detailed dynamical observables (opacity functions, products' states distributions), leading to unrealistic results. The QCT-GB procedure describes much better the detailed observables, but produces too small cross sections at low energy. The SQCT method gives a better overall agreement with QM results, including total cross sections, opacity functions and rotational distributions. In the high energy range, where QM calculations are not available, the two QCT binning methods, HB and GB, converge, and the QCT and SQCT results deviate from each other. The QCT cross sections decrease faster with growing E_{coll} than those from the SQCT calculations due to the gradual increase in importance of direct, short-lived collisions, which are partly reflected back to the reactants channel by a close range centrifugal barrier within the potential well. This dynamical effect is not contemplated in the statistical model.

Although the dynamical bias at high energy was evinced since the early studies on the kinetics of the $H^+ + H_2$ system, its actual magnitude is not entirely clear. Accurate QM calculations on the $H^+ + D_2$ isotopic variant of the reaction show that the QCT results tend to overestimate the dynamically induced decrease in the cross section. In the case of $D^+ + H_2$ considered in this work, the QM results do not stretch high enough in energy to show a marked dynamical effect. A comparison of SQCT and accurate QM results, where available, shows that the statistical model performs better for $D^+ + H_2$ than for $H^+ + D_2$, probably because the mass combination of the former reactants is more adequate than that of the latter for the initial transfer of collision energy from the ion to the molecule and thus for complex formation, which is a requisite for the validity of statistical arguments. Bearing that in mind, one can conjecture that at higher E_{coll} QM cross sections for $D^+ + H_2$ should deviate from those obtained with the SQCT method, but probably not so much as in the case of $H^+ + D_2$.

From the previous considerations we must conclude that, for all its seeming simplicity, there is possibly no satisfactory approximation able to account for all aspects of the dynamics of the title reaction. Further work would be desirable to extend the range of energies and internal states of accurate QM calculations and to delimit more precisely the applicability of current approximate treatments, both dynamical and statistical, suggesting possible improvements.

Acknowledgements

The authors would like to thank Dr Tomás González-Lezana and Dr Marlies Hankel for their collaboration in the study of these series of reactions. The authors acknowledge funding by the Spanish Ministry of Science and Innovation (grant CTQ2008-02578, FIS2007-61686, CSD2009-00038). PGJ acknowledges the FPU fellowship AP2006-03740. The research was conducted within the Unidad Asociada Química Física Molecular between the UCM and the CSIC of Spain.

References

1 J. Light, *Discuss. Faraday Soc.*, 1967, **44**, 14.
2 E. E. Nikitin, *Theory of Elementary Atomic and Molecular Processes in Gases*, Oxford University Press, New York, 1974.
3 S. Smith and J. Troe, *J. Chem. Phys.*, 1992, **97**, 5451.

4 J. Troe, *J. Chem. Soc., Faraday Trans.*, 1994, **90**, 2303.
5 E. I. Dashevskaya, A. I. Maergoirz, J. Troe, I. Litvin and E. E. Nikitin, *J. Chem. Phys.*, 2003, **118**, 7313.
6 I. G. Csizmadia, J. C. Polanyi, A. C. Roach and W. H. Wong, *Can. J. Chem.*, 1969, **47**, 4097.
7 J. R. Krenos and R. Wolfgang, *J. Chem. Phys.*, 1970, **52**, 5961.
8 K. Preston and J. C. Tully, *J. Chem. Phys.*, 1971, **54**, 4297.
9 J. C. Tully and R. K. Preston, *J. Chem. Phys.*, 1971, **55**, 562.
10 M. G. Holliday, J. T. Muckerman and L. Friedman, *J. Chem. Phys.*, 1971, **54**, 1058.
11 J. R. Krenos, R. K. Preston, R. Wolfgang and J. C. Tully, *J. Chem. Phys.*, 1974, **60**, 1634.
12 G. Ochs and E. Teloy, *J. Chem. Phys.*, 1974, **61**, 4930.
13 D. Gerlich, U. Nowotny, C. Schlier and E. Teloy, *Chem. Phys.*, 1980, **47**, 245–255.
14 D. Gerlich, in *Symposium on Atomic and surface Physics*, ed. W. Lindinger, F. Howorka, T. D. Märk and F. Egger, Institut fuer Atomphysik der Universitat Innsbruck, Innsbruk, 1982, p. 304.
15 M. J. Henchman, N. G. Adams and D. Smith, *J. Chem. Phys.*, 1981, **75**, 1201.
16 H. Villinger, M. J. Henchman and W. Lindinger, *J. Chem. Phys.*, 1982, **76**, 1590.
17 C. Schlier and U. Vix, *Chem. Phys.*, 1985, **95**, 401.
18 C. Schlier and U. Vix, *Chem. Phys.*, 1987, **113**, 211.
19 C. Schlier, U. Nowotny and E. Teloy, *Chem. Phys.*, 1987, **111**, 401–408.
20 D. Gerlich, *Adv. Chem. Phys.*, 1992, **82**, 1.
21 S. Chapman, *Adv. Chem. Phys.*, 1992, **82**, 423.
22 A. Ichihara and K. Yokoyama, *J. Chem. Phys.*, 1995, **103**, 2109.
23 A. Ichihara, T. Shirai and K. Yokoyama, *J. Chem. Phys.*, 1996, **105**, 1857.
24 M. Chajia and R. D. Levine, *Phys. Chem. Chem. Phys.*, 1999, **1**, 1205.
25 T. Takayanagi, K. Y. and A. Ichihara, *J. Chem. Phys.*, 2000, **112**, 2615.
26 C. Sanz, O. Roncero, C. Tablero, A. Aguado and M. Paniagua, *J. Chem. Phys.*, 2001, **114**, 2182.
27 A. Aguado, O. Roncero, C. Tablero, C. Sanz and M. Paniagua, *J. Chem. Phys.*, 2000, **112**, 1240.
28 H. Kamisaka, W. Bian, K. Nobusada and H. Nakamura, *J. Chem. Phys.*, 2002, **116**, 654.
29 J. G. Wang and P. C. Stancil, *Phys. Scr.*, 2002, **T96**, 72.
30 T. González-Lenzana, A. Aguado, M. Paniagua and O. Roncero, *J. Chem.Phys.*, 2005, **123**, 194309.
31 T.-S. Chu and K.-L. Han, *J. Phys. Chem. A*, 2005, **109**, 2050.
32 R.-F. Lu, T.-S. Chu and K.-L. Han, *J. Phys. Chem. A*, 2005, **109**, 6683.
33 H. Song, D. X. Dai, G. R. Wu, C. C. Wang, S. A. Harich, M. Y. Hayes, X. Y. Wang, D. Gerlich, X. M. Yang and R. T. Skodje, *J. Chem. Phys.*, 2005, **123**, 074314.
34 T. González-Lenzana, O. Roncero, P. Honvault, J.-M. Launay, N. Bulut, F. J. Aoiz and L. Bañares, *J. Chem. Phys.*, 2006, **125**, 094314.
35 L. P. Viegas, A. Alijah and A. J. C. Varandas, *J. Chem. Phys.*, 2007, **126**, 074309.
36 F. J. Aoiz, V. Sáez Rábanos, T. González-Lezana and D. E. Manolopoulos, *J. Chem. Phys.*, 2007, **126**, 161101.
37 F. J. Aoiz, T. González-Lezana and V. Sáez Rábanos, *J. Chem. Phys.*, 2007, **127**, 174109.
38 L. P. Viegas and A. J. C. Varandas, *Phys. Rev. A: At., Mol., Opt. Phys.*, 2008, **77**, 032505.
39 E. Carmona-Novillo, T. González-Lezana, O. Roncero, P. Honvault, J.-M. Launay, N. Bulut, F. J. Aoiz, L. Bañares, A. Trottier and E. Wrede, *J. Chem. Phys.*, 2008, **128**, 014304.
40 A. Zanchet, O. Roncero, T. González-Lezana, A. Rodíguez-López, A. Aguado, C. Sanz-Sanz and S. Gómez-Carrasco, *J. Phys. Chem. A*, 2009, **113**, 14488.
41 T.-S. Chu, A. J. C. Varandas and K.-L. Han, *Chem. Phys. Lett.*, 2009, **471**, 222.
42 P. G. Jambrina, F. J. Aoiz, C. J. Eyles, V. J. Herrero and V. Sáez Rábanos, *J. Chem. Phys.*, 2009, **130**, 184303.
43 P. G. Jambrina, F. J. Aoiz, N. Bulut, S. C. Smith, G. G. Balint-Kurti and M. Hankel, *Phys. Chem. Chem. Phys.*, 2010, **12**, 1102.
44 E. M. Hollmann and A. Y. Pigarov, *Phys. Plasmas*, 2002, **9**, 4330.
45 I. Méndez, F. J. Gordillo, V. J. Herrero and I. Tanarro, *J. Phys. Chem. A*, 2006, **110**, 6060.
46 E. Herbst, *Chem. Soc. Rev.*, 2001, **30**, 168.
47 E. Herbst, *J. Phys. Chem. A*, 2005, **109**, 4017.
48 W. D. Watson, *Astrophys. J.*, 1973, **181**, L129.
49 W. D. Watson, *Astrophys. J.*, 1974, **188**, 35.
50 S. S. D. Gerlich, *Planet. Space Sci.*, 2002, **50**, 1287.
51 T. J. Millar, *Astrophys. Geophys.*, 2005, **46**, 2.29.
52 R. S. Dumont and P. Brumer, *J. Phys. Chem.*, 1986, **90**, 3509.
53 M. Berblinger and C. Schlier, *J. Chem. Phys.*, 1994, **101**, 4750.
54 V. G. Ushakov, K. Nobusada and V. I. Osherov, *Phys. Chem. Chem. Phys.*, 2001, **3**, 63.
55 E. Cuervo-Reyes, J. Rubayo-Soneira, A. Aguado, M. Paniagua, C. Tablero, C. Sanz and O. Roncero, *Phys. Chem. Chem. Phys.*, 2002, **4**, 6012.
56 M. Cernei, A. Alijah and A. J. C. Varandas, *J. Chem. Phys.*, 2003, **118**, 2637.
57 L. P. Viegas, M. Cernei, A. Alijah and A. J. C. Varandas, *J. Chem. Phys.*, 2004, **120**, 253.
58 A. Saieswari and S. Kumar, *Chem. Phys. Lett.*, 2007, **449**, 358.
59 S. Amaran and S. Kumar, *J. Chem. Phys.*, 2007, **127**, 214304.
60 S. Amaran and S. Kumar, *J. Chem. Phys.*, 2008, **128**, 064301.
61 F. J. Aoiz, L. Bañares and V. J. Herrero, *J. Phys. Chem. A*, 2006, **110**, 12546.
62 E. J. Rackham, T. González-Lezana and D. E. Manolopoulos, *J. Chem. Phys.*, 2003, **119**, 12895.
63 F. J. Aoiz, T. González-Lezana and V. Sáez Rábanos, *J. Chem. Phys.*, 2008, **129**, 094305.
64 W. D. Watson, *Astrophys. J.*, 1973, **182**, L73.
65 J. H. B. A. Dalgarno and J. C. Weisheit, *Astrophys Lett.*, 1973, **14**, 77.
66 P. C. Stancil, S. Lepp and A. Dalgarno, *Astrophys. J.*, 1998, **509**, 1.
67 D. Skouteris, J. F. Castillo and D. E. Manolopoulos, *Comput. Phys. Commun.*, 2000, **133**, 128.
68 M. Hankel, S. C. Smith, R. J. Allan, S. K. Gray and G. G. Balint-Kurti, *J. Chem. Phys.*, 2006, **125**, 164303.
69 M. Hankel, S. C. Smith, S. K. Gray and G. G. Balint-Kurti, *Comput. Phys. Commun.*, 2008, **179**, 569.
70 F. J. Aoiz, V. J. Herrero and V. Sáez Rábanos, *J. Chem. Phys.*, 1992, **97**, 7423.
71 F. J. Aoiz, L. Bañares and V. J. Herrero, *J. Chem. Soc., Faraday Trans.*, 1998, **94**, 2483.
72 L. Bonnet and J.-C. Rayez, *Chem. Phys. Lett.*, 1997, **277**, 183.
73 L. Bonnet and J.-C. Rayez, *Chem. Phys. Lett.*, 2004, **397**, 106.
74 L. Bañares, F. J. Aoiz, P. Honvault, B. Bussery-Honvault and J.-M. Launay, *J. Chem. Phys.*, 2003, **118**, 565.
75 T. González-Lenzana, P. Honvault, P. G. Jambrina, F. J. Aoiz and J.-M. Launay, *J. Chem. Phys.*, 2009, **131**, 044315.